Then, the deposition chamber 519 was sufficiently evacuated, and the gate valve 511 was opened to move the substrate holder 521, which carried the substrate provided with the layers up to the first photovoltaic element 305, into the unload chamber 506 also in a manner similar to that described above.

[0088]

Then, the substrate holder 521 was taken out of the unload chamber 506 also in a manner similar to that described above.

[0089]

[Table 3]

		Gas for layer formation (cm^3/minute under normal conditions)				Power density (W/cm^2)		Pressure (Pa)	Substrate temperature(°C)	Thickness of layer (nm)
		SiH_4	H_2	PH_3 (diluted to 2% with H_2)	BF_3 (diluted to 2% with H_2)	RF	VHF			
First photovoltaic element	N2	2	48	0.5		0.04		180	225	10
	I2	2	48			0.04		150	210	500
	P2	0.025	35		1	1.2		270	165	5

[0090]

Next, the substrate provided with the layers up to the first photovoltaic element 305 was set on the anode surface of a DC magnetron sputtering apparatus, and masked with stainless steel. Indium/tin oxide was sputtered as the transparent electrode onto the substrate in a center area of a 40 by 40 mm using a target of mixed oxide of tin (10% by weight) and indium (90% by weight).

[0091]

The oxide film was deposited to a 70 nm under the conditions of substrate temperature: 170°C, argon (as an inert gas) flow rate: sccm, oxygen gas flow rate: 0.5 sccm, pressure in the deposition chamber: 300 mPa, power density on the unit target area: 0.2W/cm^2 and deposition time: about 100 seconds. Thickness of the film was estimated by the predetermined relationship between thickness and deposition time. The photovoltaic element sample thus prepared was named "Ex. 1".

[0092]

[Comparative Example 1]

A photovoltaic element was prepared in the same manner as in Example 1, except that no zinc oxide layer was placed between the first and second photovoltaic element.

[0093]

(Measurement)

First, the electrical characteristics of the zinc oxide layer deposited on the quartz substrate in Example 1 were measured. Resistivity of zinc oxide varies over a wide range (10 digits), and should be evaluated by an analysis system suitable for the resistance varying values. The 2-terminal method generally used for insulators is sensitive to contact resistance, and a resistivity meter (MCP-T600 manufactured by Dian Instruments company) based on the 4-terminal method was used, where a constant current was applied by the system including 4 terminals and 4 probes connected in series to measure a potential across and thereby resistivity. The results are given in Table 4. A zinc oxide layer prepared with the target containing a higher content of dopant and smaller quantities of charged O_2 and H_2O had a lower resistivity.

[0094]

[Table 4]

Sample No.	Resistivity (Ωcm)
A	5.0×10^{-1}
B	3.0×10^{0}
C	5.5×10^{0}
D	1.5×10^{1}
E	5.5×10^{2}
F	8.5×10^{2}
G	1.4×10^{3}
H	5.2×10^{3}
I	8.0×10^{3}
J	1.0×10^{4}

[0095]

Next, a total of 101 photovoltaic element samples prepared in each of Example 1 and Comparative Example 1 were measured for the current-voltage characteristics while they were irradiated with light under the conditions of AM1.5 spectral pattern and intensity of 100 mW/cm^2 using an analyzer (YSS-150 manufactured by Yamashita Denso company), and their short-circuit current density Jsc (mA/cm^2), open voltage Voc (V) and fill factor FF were estimated based on these characteristics to determine conversion efficiency η(%).

[0096]

Shunt resistance (Rsh) and series resistance (Rs) were also estimated based on the current-voltage

characteristics under a dark condition, where the former was defined as slope near V=0, and the latter as slope of current when it rose up.

[0097]

The results are given in Tables 5, 6, 7 and 8, respectively.

The zinc oxide layer having a higher resistivity on the second photovoltaic element side and a lower resistivity on the first photovoltaic element side can improve FF level, increase photocurrent and improve conversion efficiency for the stacked photovoltaic element by increasing reflection, reducing short-circuit current and improving the joint surface. On the other hand, the layer having a reversed combination of resistivity deteriorates in conversion efficiency as the Jsc value decreases. Moreover, the layer having the former resistivity combination exhibits excellent characteristics, when its resistivity is in a range from 2×10^0 Ωcm to 5×10^3 Ωcm. However, it deteriorates in conversion efficiency when its resistivity is below 2×10^0 Ωcm or the high resistivity portion has 5×10^2 Ωcm or less, resulting in decreased shunt resistance by short-circuit current, which in turn causes decreased FF value and then Jsc level. Resistivity exceeding 5×10^3 Ωcm, on the other hand, slightly reduces the conversion efficiency, resulting from increased series resistance.

[0098]

[Table 5]

Conversion efficiency		First zinc oxide layer									
		A	B	C	D	E	F	G	H	I	J
Second zinc oxide layer	Comparative Example 1	0.943									
	A	0.971	0.969	0.972	0.973	0.971	0.981	0.978	0.977	0.973	0.972
	B	0.970	0.972	0.975	0.972	0.976	0.980	0.981	0.982	0.981	0.978
	C	0.985	0.981	0.982	0.983	0.981	0.981	0.982	0.982	0.982	0.980
	D	0.973	0.980	0.983	0.983	0.984	0.985	0.985	0.986	0.986	0.985
	E	0.974	0.982	1.105	1.053	1.002	0.988	0.978	0.980	0.990	0.986
	F	0.982	0.990	1.101	1.110	1.058	1.015	0.991	0.992	0.990	0.990
	G	0.985	0.992	1.102	1.102	1.169	1.140	1.011	0.987	0.991	0.996
	H	0.983	0.993	1.103	1.110	1.089	1.088	1.090	1.005	0.958	0.980
	I	0.988	0.990	0.995	0.996	0.998	0.992	0.994	0.993	0.991	0.990
	J	0.986	0.987	0.991	0.992	0.995	0.991	0.993	0.991	0.990	0.989

[0099]

[Table 6]

JSC		First zinc oxide layer									
		A	B	C	D	E	F	G	H	I	J
Second zinc oxide layer	Comparative Example 1	0.960									
	A	0.971	0.969	0.972	0.973	0.971	0.981	0.978	0.977	0.973	0.972
	B	0.970	0.972	0.975	0.972	0.976	0.980	0.981	0.982	0.981	0.978
	C	0.985	0.981	0.982	0.983	0.981	0.981	0.982	0.982	0.982	0.980
	D	0.973	0.980	0.983	0.983	0.984	0.985	0.985	0.986	0.986	0.985
	E	0.974	0.982	1.105	1.053	1.002	0.988	0.978	0.980	0.990	0.986
	F	0.982	0.990	1.101	1.110	1.058	1.015	0.991	0.992	0.990	0.990
	G	0.985	0.992	1.102	1.102	1.169	1.140	1.011	0.987	0.991	0.996
	H	0.983	0.993	1.103	1.110	1.089	1.088	1.090	1.005	0.958	0.980
	I	0.988	0.990	0.995	0.996	0.998	0.992	0.994	0.993	0.991	0.990
	J	0.986	0.987	0.991	0.992	0.995	0.991	0.993	0.991	0.990	0.989

[0100]

[Table 7]

Shunt resistance		First zinc oxide layer									
		A	B	C	D	E	F	G	H	I	J
Second zinc oxide layer	A	0.956	0.955	0.960	0.954	0.946	0.952	0.953	0.954	0.956	0.963
	B	0.963	0.972	0.974	0.978	0.985	0.989	0.988	0.987	0.986	0.990
	C	0.978	0.979	0.982	0.981	0.984	0.992	0.991	0.993	0.990	0.994
	D	0.985	0.989	0.990	0.992	0.991	0.989	0.992	0.996	0.993	0.994
	E	1.001	1.000	1.002	1.010	1.005	1.008	1.005	1.010	1.015	1.053
	F	0.996	0.999	1.003	1.002	1.003	1.010	1.005	1.015	1.045	1.060
	G	0.999	0.996	1.005	1.003	1.020	1.010	1.011	1.022	1.065	1.121
	H	0.999	1.002	1.004	1.005	1.009	1.015	1.019	1.030	1.089	1.156
	I	1.001	1.003	1.008	1.006	1.010	1.011	1.069	1.155	1.120	1.188
	J	1.010	1.011	1.009	1.010	1.011	1.023	1.088	1.145	1.165	1.190

[0101]

[Table 8]

Series resistance		First zinc oxide layer									
		A	B	C	D	E	F	G	H	I	J
Second zinc oxide layer	A	0.989	0.989	0.989	0.992	0.994	0.995	0.999	0.999	1.098	1.200
	B	0.990	0.991	0.994	0.999	0.999	1.001	1.000	1.002	1.090	1.201
	C	0.993	0.995	0.998	1.002	1.001	0.998	0.999	1.000	1.082	1.205
	D	0.996	0.996	0.999	0.997	0.989	0.992	1.001	1.003	1.102	1.197
	E	0.995	0.988	0.996	0.995	1.002	1.003	1.009	1.100	1.152	1.199
	F	0.993	0.991	0.997	1.020	1.001	1.005	1.012	1.120	1.135	1.140
	G	0.989	0.996	0.999	1.002	1.002	1.005	1.015	1.153	1.190	1.250
	H	0.989	0.999	0.999	1.011	1.010	1.010	1.015	1.160	1.203	1.203
	I	1.025	1.060	1.055	1.068	1.088	1.101	1.105	1.169	1.170	1.201
	J	1.150	1.155	1.102	1.100	1.111	1.056	1.177	1.188	1.165	1.250

[0102]

*In the above-described relative series resistance, a larger numeral represents a higher series resistance. The electrical properties deteriorate as series resistance increases.

[0103]

[Example 2]

A stacked photovoltaic element was prepared in a manner similar to that for Example 1, by using a pin-type photovoltaic element 302 with the i-layer of intrinsic microcrystalline Si as the second photovoltaic element, a pin-type photovoltaic element 305 with the i-layer of intrinsic amorphous Si:H as the first photovoltaic element, and an intermediate layer of zinc oxide (refer to Fig. 3).

[0104]

The zinc oxide layer sample was prepared separately from the photovoltaic element on a quartz substrate, where the same Al-containing target was used, and charge rates of oxygen gas and vaporized H_2O gas were adjusted to have a varying electric conductivity (Table 9). Based on these results, the conditions were found to prepare the zinc oxide layer having resistivity gradually changing in the thickness direction of the layer, so-called graded resistivity.

[0105]

The stacked photovoltaic element with the intermediate layer of zinc oxide was prepared in the

same manner as in Example 1, except that the zinc oxide layer was prepared under the conditions given in Table 10, where these conditions were adjusted to give zinc oxide resitivity increasing from the first photovoltaic element side towards the second photovoltaic element side.

[0106]

The stacked photovoltaic element samples thus prepared (Ex. 2-1 to 2-5) were evaluated in the same manner as in Example 1. The results are also given in Table 10.

[0107]

[Table 9]

Sample No.	Resistivity (Ωcm)
A	5.0×10^{-1}
B	5.0×10^{0}
C	2.5×10^{1}
D	5.5×10^{1}
E	5.5×10^{3}
F	5.0×10^{3}
G	7.5×10^{3}

[0108]

[Table 10]

Element No.	Resistivity range	Conversion efficiency
Ex. 2-1	5.0×10^{0}-5.0×10^{3}	1.000
Ex. 2-2	5.0×10^{2}-5.0×10^{3}	1.010
Ex. 2-3	5.0×10^{0}-4.0×10^{2}	0.979
Ex. 2-4	5.0×10^{-1}-1.0×10^{3}	0.985
Ex. 2-5	5.0×10^{0}-7.5×10^{3}	0.987

[0109]

It is found also in Example 2 that the zinc oxide layer having a higher resistivity on the second photovoltaic element side and a lower resistivity on the first photovoltaic element side can increase reflection, improve short-circuit current and improve the joint surface of the stacked element, to improve its FF level, photocurrent and conversion efficiency, even when resistivity increases in a graded manner.

[0110]

It is also found that the effective resistivity range is 2×10^{0} Ωcm or more and 5×10^{3} Ωcm or less, and high resistivity range is 5×10^{2} Ωcm or more.

[0111]

[Example 3]

In Example 3, the stacked photovoltaic element of the third aspect of the present invention comprising a pin-type photovoltaic element with the i-type layer of intrinsic amorphous Si:H as the first photovoltaic

element, a pin-type photovoltaic element with the i-type layer of intrinsic microcrystalline Si as the second photovoltaic element, and an intermediate layer of indium/tin oxide and zinc oxide was produced as shown in Fig. 8.

[0112]

Referring to Fig. 8, the substrate 801, 45 mm square and 0.15 mm thick, was of flat stainless steel (SUS 430), commonly referred to as BA-finished one. It was put in a commercial DC magnetron sputtering unit (not shown), which was evacuated to a pressure of 10^{-3} Pa or less.

[0113]

Argon was supplied into the unit at 30 cm^3/min (normal conditions) to keep pressure inside at 2×10^{-1} Pa. A DC power of 120 W was applied to an aluminum target (diameter: 6 inches) for 90 seconds to form a thin film of aluminum with a thickness of 70 nm on the substrate, while the substrate was kept unheated. Then, a DC power of 500 W was applied to a zinc oxide target (diameter: 6 inches), after the electrical connection was changed, for 30 minutes to form the increased reflectance layer of zinc oxide with a thickness of about 3000 nm on the substrate 801, while the substrate was kept at 200°C.

[0114]

The deposited film forming apparatus 500,

schematically illustrated in Fig. 5, was used to form the photovoltaic elements under the given deposition conditions given in Table 11.

[0115]

[Table 11]

		Gas for layer formation (cm^3/minute under normal conditions)				Power density (W/cm^2)		Pressure (Pa)	Substrate temperature (°C)	Thickness of layer (nm)
		SiH_4	H_2	PH_3 (diluted to 2% with H_2)	BF_3 (diluted to 2% with H_2)	RF	VHF			
First photovoltaic element	N1	2	48	0.5		0.04		180	225	10
	I1	2	48			0.04		150	210	500
	P1	0.025	35		1	1.2		270	165	5
Second photovoltaic element	N2	2	48	0.5		0.04		180	225	20
	I2	25	750				0.2	40	250	2000
	P2	0.025	35		1	1.2		270	165	5

[0116]

First, the second photovoltaic element was formed on the substrate 801 under the conditions given in Table 11 by the following procedure. The substrate 801 was set on the substrate holder 521 and then on the rail 520 in the load chamber 501. The load chamber 501 was then evacuated to a vacuum of several hundreds mPa or less.

[0117]

Next, the gate valve 507 was opened, and the substrate holder 521 was moved into the deposition chamber 515 for depositing the n-type layer in the chamber 502, where the n-type layer was deposited to a given thickness using a given feed gas, while the gate valves 507, 508, 509, 510 and 511 were kept closed. The chamber 502 was sufficiently evacuated, and the gate valve 508 was opened to move the substrate holder 521 into the deposition chamber 503. Then the gate valve 508 was closed.

[0118]

The substrate was heated to a given temperature by the heater 512, and a necessary quantity of the feed gas was charged in the chamber. Given microwave or VHF energy was introduced into the deposition chamber 513, which was evacuated to a given vacuum level, to generate a plasma therein to deposit the i-type layer of microcrystalline silicon to a given thickness on the

substrate. The chamber 503 was sufficiently evacuated, and the gate valves 509 and 510 were opened to move the substrate holder 521 from the chamber 503 to the chamber 505.

[0119]

After the substrate holder 521 was moved into the deposition chamber 519 for depositing the p-type layer in the chamber 505, the substrate was heated to a given temperature by the heater 518. A necessary quantity of the feed gas to deposit the p-type layer was charged in the deposition chamber 519, in which RF energy was supplied to deposit the p-type layer to a given thickness, while the chamber was kept at a given vacuum level.

[0120]

Similarly, the chamber 519 was sufficiently evacuated, and the gate valve 511 was opened to move the substrate holder 521 having the substrate 201 with a stacked photovoltaic element into the unload chamber 506.

[0121]

Then, the substrate was cooled with nitrogen gas charged in the unload chamber 506, while all of the gate valves were closed. Then, the substrate holder 521 was taken out of the unload chamber 506, after the discharge valve was opened.

[0122]

Next, the substrate 801, on which the layers up to the second photovoltaic element were formed, was removed from the substrate holder 521 and set in a commercial DC magnetron sputtering apparatus (not shown) in order to form the immediate layer. Then, the apparatus was evacuated to a pressure of 10^{-3} Pa or less.

[0123]

Indium/tin oxide was sputtered onto the substrate with a mixed of tin oxide (3% by weight) and indium oxide (97% by weight) as the target.

[0124]

It was deposited under the conditions of substrate temperature: 170°C, argon gas (as an inert gas) flow rate: 50 cm^3/minute (normal conditions), oxygen gas flow rate: 0.2 cm^3/minute (normal conditions) and pressure in the deposition chamber: 200 mPa, where a DC power of 10 W was applied for about 100 seconds to deposit the layer to a thickness of about 10 nm after the electrical connection was changed to the indium/tin oxide target (diameter: 6 inches). Thickness of the layer was estimated by the predetermined relationship between thickness and deposition time.

[0125]

Then, the zinc oxide layer was deposited by sputtering in the same apparatus, after the target was changed to that of zinc oxide.

[0126]

It was deposited under the conditions of argon gas flow rate: 30 cm^3/minute (normal conditions), oxygen gas flow rate: 2 cm^3/minute (normal conditions) and pressure in the deposition chamber: 2×10^{-1} Pa, where a DC power of 100 W was applied for about 5 minutes to deposit the zinc oxide layer to a thickness of about 100 nm, after the electrical connection was changed to the zinc oxide target (diameter: 6 inches) and the substrate was heated to 120°C.

[0127]

The deposited film forming apparatus 500, schematically illustrated in Fig. 5, was again used to form the pin-type photovoltaic element of amorphous Si:H as the first photovoltaic element on the substrate 801 provided with the intermediate layer by the following procedure.

[0128]

The n-type layer was deposited to a given thickness under given conditions in the chamber 502 in a manner similar to that described above. The gate valves 508 and 509 were opened, after the chamber 502 was sufficiently evacuated, and the substrate holder 521 was moved into the chamber 504. Then, these valves were closed.

[0129]

The substrate was heated to a given temperature by

the heater 516, and a necessary quantity of the feed gas was charged in the chamber. Given RF energy was introduced into the deposition chamber 517, which was evacuated to a given vacuum level, to generate a plasma therein to deposit the i-type layer of amorphous Si:H to a given thickness. The chamber 504 was sufficiently evacuated, and the gate valve 510 was opened to move the substrate holder 521 from the chamber 504 to the chamber 505.

[0130]

The p-type layer was deposited to a given thickness in the chamber 505 in a manner similar to that described above.

[0131]

Similarly, the deposition chamber 519 was sufficiently evacuated, and the gate valve 511 was opened to move the substrate holder 521, which supported the substrate 801 provided with the photovoltaic element, into the unload chamber 506.

[0132]

Then, the substrate holder 521 was taken out of the unload chamber 506 in a manner similar to that described above.

[0133]

Next, the substrate was set on the anode surface of a DC magnetron sputtering apparatus, and masked with stainless steel. Indium/tin oxide was sputtered onto

the substrate in a center area of a 40 by 40 mm from a target composed of tin oxide (10% by weight) and indium oxide (90% by weight) as the transparent electrode.

[0134]

The oxide film was deposited to 70 nm under the conditions of substrate temperature: 170°C, argon (as an inert gas) flow rate: 50 cm^3/minute (normal conditions), oxygen gas flow rate: 0.5 cm^3/minute (normal conditions), pressure in the deposition chamber: 300 mPa, power density on the unit target area: 0.2W/cm^2 and deposition time: about 100 seconds. Thickness of the film was estimated by the predetermined relationship between thickness and deposition time. The stacked photovoltaic element sample thus prepared was named "Ex. 3".

[0135]

[Comparative Example 2]

The stacked photovoltaic element 1200 was prepared to have the same structure as that of the stacked photovoltaic element 800 of the present invention (Fig. 8), except that the intermediate layer 1206 was composed of only one layer as shown in Fig. 12. Referring to Fig. 12, on the electroconductive substrate 1201 of a metal or the like, the light reflection layer 1202, second photovoltaic element 1203, intermediate layer 1206, first photovoltaic element 1207 and transparent electrode 1208 were

stacked in this order.

[0136]

The zinc oxide layer as the intermediate layer 1206 was deposited by sputtering with a target of zinc oxide.

[0137]

It was deposited under the conditions of argon gas flow rate: 30 cm^3/minute (normal conditions), oxygen gas flow rate: 2 cm^3/minute (normal conditions) and pressure in the deposition chamber: 2×10^{-1} Pa, where a DC power of 100 W was applied for about 5 minutes and 30 seconds to deposit the zinc oxide layer to a thickness of about 110 nm, after the electrical connection was changed to the zinc oxide target (diameter: 6 inches) and the substrate was heated to 100°C. The stacked photovoltaic element was prepared in the same manner as in Example 3, except that the intermediate layer 1206 composed of only one layer was used. This sample was named "Compar. 2-1".

[0138]

In deposition of the intermediate layer 1206, indium/tin oxide was sputtered onto the substrate using a target composed of tin oxide (3% by weight) and indium oxide (97% by weight).

[0139]

The intermediate layer was deposited to about 110 nm under the conditions of substrate temperature:

170°C, argon (as an inert gas) flow rate: 50 cm^3/minute (normal conditions), oxygen gas flow rate: 0.2 cm^3/minute (normal conditions), pressure in the deposition chamber: 200 mPa, where a DC power of 10 W was applied for about 18 minutes and 20 seconds, after the electrical connection was changed to the target of indium/tin oxide (diameter: 6 inches). The stacked photovoltaic element was prepared in the same manner as in Example 3, except that the intermediate layer 1206 prepared above was used. This sample was named "Compar. 2-2".

[0140]

Moreover, in preparation of the intermediate layer 806 for the stacked photovoltaic element 800 illustrated in Fig. 8, zinc oxide was sputtered first with a target of zinc oxide.

[0141]

It was deposited under the conditions of argon gas flow rate: 30 cm^3/minute (normal conditions), oxygen gas flow rate: 2 cm^3/minute (normal conditions) and pressure in the deposition chamber: 2×10^{-1} Pa, where a DC power of 100 W was applied for about 30 minutes to deposit the zinc oxide layer to a thickness of about 10 nm, after the electrical connection was changed to the zinc oxide target (diameter: 6 inches) and the substrate was heated to 120°C.

[0142]

Then, indium/tin oxide was sputtered in the same apparatus, after the target was changed to a target composed of tin oxide (3% by weight) and indium oxide (97% by weight).

[0143]

The intermediate layer was deposited to about 100 nm under the conditions of substrate temperature: 170°C, argon (as an inert gas) flow rate: 50 cm^3/minute (normal conditions), oxygen gas flow rate: 0.2 cm^3/minute (normal conditions), pressure in the deposition chamber: 200 mPa, where a DC power of 10 W was applied for about 16 minutes and 40 seconds, after the electrical connection was changed to the target of indium/tin oxide (diameter: 6 inches). The stacked photovoltaic element was prepared in the same manner as in Example 3, except that the intermediate layer prepared above was used. This sample was named "Compar. 2-3".

[0144]

These samples prepared in Example 3 and Comparative Example 2 were measured for the current-voltage characteristics while they were irradiated with light under the conditions of AM1.5 spectral pattern and intensity of 100 mW/cm^2 using an analyzer (YSS-150 manufactured by Yamashita Denso company), and their short-circuit current density Jsc (mA/cm^2), open voltage Voc (V) and fill factor FF were estimated based

on these characteristics to determine conversion efficiency η(%).

[0145]

Shunt resistance Rsh (kΩcm^2) was also estimated based on the current-voltage characteristics under a dark condition from the slope at near the origin.

[0146]

These results are given in Table 12 by the ratio of characteristic values of Example to those of Comparative Example (Ex. 3/Compar. 2-1, Ex. 3/Compar. 2-2 and Ex. 3/Compar. 2-3).

[0147]

[Table 12]

	Jsc	FF	Voc	Eff.	Rsh
Ex. 3/ Compar. 2-1	1.001	1.017	1.044	1.064	8.20×10^{-1}
Ex. 3/ Compar. 2-2	1.014	1.152	1.006	1.174	1.54×10^{2}
Ex. 3/ Compar. 2-3	1.013	1.156	1.051	1.231	9.23×10^{1}

[0148]

Ex. 3 exhibited a higher conversion efficiency than Compar. 2-1 resulting from improvements both in the FF and Voc values. Fig. 10 shows JV curves of these samples. Superiority of Ex. 3 mainly resulted from the improved Voc value, conceivably indicating that Compar. 2-1 had a defective junction between the

interface with the semiconductor and that with the intermediate layer.

[0149]

Ex.3 exhibited a higher conversion efficiency than Compar. 2-2 resulting from improvements in all of the FF, Voc and Rsh values. Fig. 11 shows JV curves of these samples. Superiority of Ex. 3 mainly resulted from decreased shunt resistance of Compar. 2-2, which mainly decreased the FF value.

[0150]

Ex. 3 exhibited a higher conversion efficiency than Compar. 2-3 resulting from improvements in all of the FF, Voc and Rsh values. Compar. 3 was formed by depositing zinc oxide and then indium/tin oxide in this order which was reversed in Ex. 3. This order conceivably deteriorated the interfacial junction conditions and shunt resistance, which in turn caused the decreased Voc and FF values.

[0151]

The reliability test was conducted by the following procedure. A reverse bias of -0.85 V was applied continuously for 20 hours to the sample kept at 85°C and 85% RH in a high-temperature, high-humidity chamber. It was then taken out of the chamber, and naturally dried and cooled sufficiently to be analyzed for the voltage-current characteristics. The results are given in Table 13, where each of the

characteristics reported is relative to the initial level.

[0152]

[Table 13]

	Jsc	FF	Voc	Eff.	Rsh
Ex. 3	1.001	0.991	0.997	0.989	0.785
Compar. 2-1	1.000	0.989	0.998	0.987	0.779
Compar. 2-2	0.959	0.906	0.992	0.862	0.387
Compar. 2-3	0.980	0.947	0.995	0.924	0.449

[0153]

The reliability test caused essentially no decrease in shunt resistance with respect to both Ex. 3 and Compar. 2-1, whereas it decreased the value from the initial level with respect to Compar. 2-2 and 2-3, mainly resulting in the decreased Voc and FF values to cause deteriorated photoelectric conversion efficiency.

[0154]

It is therefore concluded, based on the above results, that the second and third aspect of the present invention have good initial photoelectric conversion efficiency and are highly durable.

[0155]

[Example 4]

In Example 4, the stacked photovoltaic element of the third aspect of the present invention comprising the pin-type photovoltaic element with the i-type layer of intrinsic amorphous Si:H as the first photovoltaic

element, pin-type photovoltaic element with the i-type layer of intrinsic microcrystalline Si as the second photovoltaic element, and the intermediate layer of indium/tin oxide and zinc oxide , as shown in Fig. 8, was produced, where three samples of varying the thickness ratio of the indium/tin oxide layer to zinc oxide layer were prepared.

[0156]

For preparation of the intermediate layer, indium/tin oxide was sputtered onto the substrate using a target composed of tin oxide (3% by weight) and indium oxide (97% by weight).

[0157]

Indium/tin oxide was deposited under the conditions of substrate temperature: 170°C, argon gas (as an inert gas) flow rate: 50 cm^3/minute (normal conditions), oxygen gas flow rate: 0.2 cm^3/minute (normal conditions) and pressure in the deposition chamber: 200 mPa, where a DC power of 10 W was put for a given time to deposit the layer to a given thickness after the electrical connection was changed to the indium/tin oxide target (diameter: 6 inches).

[0158]

Then, the zinc oxide layer was deposited by sputtering in the same apparatus, after the target was changed to that of zinc oxide.

[0159]

Zinc oxide was deposited under the conditions of argon gas flow rate: 30 cm^3/minute (normal conditions), oxygen gas flow rate: 2 cm^3/minute (normal conditions) and pressure in the deposition chamber: 2×10^{-1} Pa, where a DC power of 100 W was applied for a given time to deposit the layer to a given thickness, after the electrical connection was changed to the zinc oxide target (diameter: 6 inches) and the substrate was heated to 120°C. All of these intermediate layers have the same total thickness set at about 110 nm

[0160]

These stacked photovoltaic element samples were prepared in the same manner as in Example 3, except that thickness ratio of the indium/tin oxide layer to zinc oxide layer was varied. These samples were named "Ex. 4A", "Ex. 4B", "Ex. 4C" and "Ex. 4D". Table 14 summarizes the conditions under which each sample was prepared.

[0161]

[Table 14]

	Indium tin oxide		Zinc oxide	
	Deposition time	Thickness of layer (nm)	Deposition time	Thickness of layer (nm)
Ex. 4A	1 min. 40 sec.	10	5 min.	100
Ex. 4B	7 min. 30 sec.	45	3 min. 15 sec.	65
Ex. 4C	10 min. 50 sec.	65	2 min. 15 sec.	45
Ex. 4D	16 min. 40 sec.	100	30 sec.	10

[0162]

Next, each photovoltaic element was analyzed for its current-voltage characteristics in the same manner as in Example 3. The results are given in Table 15, where each of the characteristics is relative to that of Compar. 2-2.

[0163]

[Table 15]

	Jsc	FF	Voc	Eff.	Rsh
Ex. 4A/ Compar. 2-2	1.014	1.152	1.006	1.174	1.54×10^{2}
Ex. 4B/ Compar. 2-2	1.013	1.147	1.006	1.169	3.11×10^{1}
Ex. 4C/ Compar. 2-2	1.010	1.078	1.001	1.090	1.57×10^{1}
Ex. 4D/ Compar. 2-2	1.009	1.023	0.999	1.031	2.18×10^{0}

[0164]

Each of Ex. 4A, Ex. 4B, Ex. 4C and Ex. 4D had better characteristics than Compar. 2-2. It was also observed that conversion efficiency increased as the thickness of the indium/tin oxide layer became smaller than that of the zinc oxide layer. The reliability test was also conducted in the same manner as in Example 3. The results are given in Table 16, where each of the characteristics reported is relative to the initial level.

[0165]

[Table 16]

	Jsc	FF	Voc	Eff.	Rsh
Ex. 4A	1.001	0.991	0.997	0.989	0.785
Ex. 4B	0.999	0.997	1.000	0.996	0.899
Ex. 4C	0.982	0.910	1.000	0.894	0.240
Ex. 4D	0.963	0.903	0.999	0.870	0.298
Compar. 2-2	0.959	0.906	0.992	0.862	0.387

[0166]

The reliability test results indicated that each of Ex. 4A, Ex. 4B, Ex. 4C and Ex. 4D had higher reliability than Compar. 2-2. It was also observed that reliability increased as the thickness of the indium/tin oxide layer became smaller than that of the zinc oxide layer.

[0167]

To summarize these results: Ex. 4A and Ex. 4B have a higher conversion efficiency and higher reliability than Ex. 4C and Ex. 4D, and the indium/tin oxide layer is preferably thinner than the zinc oxide layer.

[0168]

[Example 5]

In Example 5, the stacked photovoltaic element of the third aspect of the present invention comprising the pin-type photovoltaic element with the i-type layer of intrinsic amorphous Si:H as the first photovoltaic element, the pin-type photovoltaic element with the i-type layer of intrinsic microcrystalline Si as the

second photovoltaic element, and the intermediate layer of indium/tin oxide and zinc oxide, as shown in Fig. 8, was produced, where four samples of varying the thickness ratio of the indium/tin oxide layer to zinc oxide layer were prepared.

[0169]

For preparation of the intermediate layer, indium/tin oxide was sputtered onto the substrate using a target composed of tin oxide (3% by weight) and indium oxide (97% by weight).

[0170]

Indium/tin oxide was deposited under the conditions of substrate temperature: 170□C, argon gas (as an inert gas) flow rate: 50 cm^3/minute (normal conditions), oxygen gas flow rate: 0.2 cm^3/minute (normal conditions) and pressure in the deposition chamber: 200 mPa, where a DC power of 10 W was put for a given time to deposit the layer to a given thickness after the electrical connection was changed to the indium/tin oxide target (diameter: 6 inches).

[0171]

Then, the zinc oxide layer was deposited by sputtering in the same apparatus, after the target was changed to that of zinc oxide.

[0172]

Zinc oxide was deposited under the conditions of argon gas flow rate: 30 cm^3/minute (normal conditions),

oxygen gas flow rate: 2 cm^3/minute (normal conditions) and pressure in the deposition chamber: 2×10^{-1} Pa, where a DC power of 100 W was applied for 5 minutes to deposit the layer to a thickness of 100 nm, after the electrical connection was changed to the zinc oxide target (diameter: 6 inches) and the substrate was heated to 120°C. These stacked photovoltaic element samples were prepared in the same manner as in Example 3, except that thickness of the indium/tin oxide layer for the intermediate layer was varied. These samples were named "Ex. 5A", "Ex. 5B", "Ex. 5C" and "Ex. 5D". Table 17 summarizes the conditions under which each sample was prepared.

[0173]

[Table 17]

	Indium tin oxide	
	Deposition time	Thickness of layer (nm)
Ex. 5A	1 min. 40 sec.	10
Ex. 5B	5	0.5
Ex. 5C	10 sec.	1
Ex. 5D	8 min. 20 sec.	50
Ex. 5E	10 min. 50 sec.	65

[0174]

Next, each photovoltaic element was analyzed for its current-voltage characteristics in the same manner as in Example 3. The results are given in Table 18,

where each of the characteristics is relative to that of Compar. 2-2.

[0175]

[Table 18]

	Jsc	FF	Voc	Eff.	Rsh
Ex. 5A/ Compar. 2-2	1.001	1.017	1.044	1.064	8.20×10^{-1}
Ex. 5B/ Compar. 2-2	1.002	1.006	1.017	1.025	9.83×10^{-1}
Ex. 5C/ Compar. 2-2	1.005	1.011	1.028	1.044	8.37×10^{-1}
Ex. 5D/ Compar. 2-2	1.008	1.012	1.040	1.062	6.90×10^{-1}
Ex. 5E/ Compar. 2-2	1.008	0.997	1.040	1.045	5.82×10^{-1}

[0176]

Each of Ex. 5A, Ex. 5B, Ex. 5C and Ex. 5D had better characteristics than Compar. 2-2. It was also observed that the indium/tin oxide layer having a thickness in a range from 1 to 50 nm gave the stacked photovoltaic element of higher conversion efficiency. The reliability test was also conducted in the same manner as in Example 3. The results are given in Table 19, where each of the characteristics reported is relative to the initial level.

[0177]

[Table 19]

	Jsc	FF	Voc	Eff.	Rsh
Ex. 5A	1.001	0.991	0.997	0.989	0.785
Ex. 5B	0.998	0.992	0.998	0.988	0.800
Ex. 5C	0.999	0.994	0.997	0.990	0.778
Ex. 5D	0.999	0.974	1.001	0.974	0.832
Ex. 5E	0.997	0.969	1.000	0.966	0.604

[0178]

The reliability test results indicated that each of Ex. 5A, Ex. 5B, Ex. 5C and Ex. 5D deteriorated in these characteristics to a limited extent. The thinner indium/tin oxide layer gave the stacked photovoltaic element of higher reliability. The indium/tin oxide layer is preferably 50 nm thick or less.

[0179]

To summarize these results: the indium/tin oxide layer having a thickness in a range from 1 to 50 nm gives the stacked photovoltaic element of higher conversion efficiency and reliability.

[0180]

[Example 6]

In Example 6, the stacked photovoltaic element of the third aspect of the present invention comprising the pin-type photovoltaic element with the i-type layer of intrinsic amorphous Si:H as the first photovoltaic element, the pin-type photovoltaic element with the i-type layer of intrinsic microcrystalline Si as the second photovoltaic element and the intermediate layer

of indium/tin oxide and zinc oxide as shown in Fig. 8, was produced where two samples were prepared under different conditions.

[0181]

For preparation of the intermediate layer, indium/tin oxide was sputtered onto the substrate using a target composed of tin oxide (3% by weight) and indium oxide (97% by weight).

[0182]

Indium/tin oxide was deposited under the conditions of substrate temperature: 170°C, argon gas (as an inert gas) flow rate: 50 cm^3/minute (normal conditions), oxygen gas flow rate: 0.2 cm^3/minute (normal conditions) and pressure in the deposition chamber: 200 mPa, where a DC power of 10 W was applied for 8 minutes and 20 seconds to deposit the layer to a thickness of 50 nm, after the electrical connection was changed to the indium/tin oxide target (diameter: 6 inches).

[0183]

Then, the zinc oxide layer was deposited by sputtering in the same apparatus, after the target was changed to that of zinc oxide.

[0184]

Zinc oxide was deposited under the conditions of argon gas flow rate: 30 cm^3/minute (normal conditions), oxygen gas flow rate: 2 cm^3/minute (normal conditions)

and pressure in the deposition chamber: 2×10^{-1} Pa, where a DC power of 100 W was applied for 5 minutes to deposit the layer to a thickness of 100 nm, after the electrical connection was changed to the zinc oxide target (diameter: 6 inches) and the substrate was heated to 120°C. These stacked photovoltaic element samples were prepared in the same manner as in Example 3, except that thickness of the indium/tin oxide layer for the intermediate layer was varied. This sample was named “Ex. 6A”.

[0185]

In a similar manner, a DC power of 35 W was applied for 2 minutes and 30 seconds to deposit the layer to a thickness of 50 nm, after the electrical connection was changed to the indium/tin oxide target, and then a DC power of 30 W was put for 16 minutes and 40 seconds to deposit the zinc oxide layer to a thickness of 100 nm, after the electrical connection was changed to the zinc oxide target. This sample was named “Ex. 6B”. Each sample was analyzed for its current-voltage characteristics in the same manner as in Example 3. The results are given in Table 20, where each of the characteristics is relative to that of Compar. 2-2.

[0186]

[Table 20]

	Jsc	FF	Voc	Eff.	Rsh
Ex. 6A/ Compar. 2-2	1.020	1.147	1.002	1.172	1.29×10^2
Ex. 6B/ Compar. 2-2	1.020	1.133	0.996	1.151	1.57×10^2

[0187]

Ex. 6A had better characteristics than Ex.6B. The reliability test was also conducted in the same manner as in Example 3. The results are given in Table 21, where each of the characteristics reported is relative to the initial level.

[0188]

[Table 21]

	Jsc	FF	Voc	Eff.	Rsh
Ex. 6A	0.999	0.974	1.001	0.974	0.832
Ex. 6B	0.998	0.978	0.998	0.974	0.834
Compar. 2-2	0.959	0.906	0.992	0.862	0.387

[0189]

Both samples produced the good results in the reliability test.

[0190]

To summarize these results: a higher conversion efficiency and reliability can be realized, when the indium/tin oxide layer is deposited at a lower rate than the zinc oxide layer.

[0191]

[Example 7]

In Example 7, the stacked photovoltaic element of the third aspect of the present invention comprising the pin-type photovoltaic element with the i-type layer of intrinsic amorphous Si:H as the first photovoltaic element, the pin-type photovoltaic element with the i-type layer of intrinsic microcrystalline Si as the second photovoltaic element, and the intermediate layer of indium/tin oxide and zinc oxide, as shown in Fig. 8, was produced where three samples were prepared under different conditions.

[0192]

For preparation of the intermediate layer, indium/tin oxide was sputtered onto the substrate using a target composed of tin oxide (3% by weight) and indium oxide (97% by weight).

[0193]

Indium/tin oxide was deposited under the conditions of substrate temperature: 170°C, argon gas (as an inert gas) flow rate: 50 cm^3/minute (normal conditions), oxygen gas flow rate: 0.2 cm^3/minute (normal conditions) and pressure in the deposition chamber: 200 mPa, where a DC power of 10 W was put for 8 minutes and 100 seconds to deposit the layer to a thickness of 10 nm, after the electrical connection was changed to the indium/tin oxide target (diameter: 6 inches).

[0194]

Then, the zinc oxide layer was deposited by sputtering in the same apparatus, after the target was changed to that of zinc oxide.

[0195]

Zinc oxide was deposited under the conditions of argon gas flow rate: 30 cm^3/minute (normal conditions), oxygen gas flow rate: 2 cm^3/minute (normal conditions) and pressure in the deposition chamber: 2×10^{-1} Pa, where a DC power of 100 W was applied for 5 minutes to deposit the layer to a thickness of 100 nm, after the electrical connection was changed to the zinc oxide target (diameter: 6 inches) and the substrate was heated to 120°C. These stacked photovoltaic element samples were prepared in the same manner as in Example 3, except that thickness of the indium/tin oxide layer for the intermediate layer was varied. This sample was named "Ex. 7A".

[0196]

In a similar manner, a DC power of 10 W was applied for 100 seconds to deposit the indium/tin oxide layer to a thickness of 10 nm while the substrate was kept at 120°C, after the electrical connection was changed to the indium/tin oxide target, and then a DC power of 100 W was put for 5 minutes to deposit the zinc oxide layer to a thickness of 100 nm, after the electrical connection was changed to the zinc oxide

target and the substrate was heated to 170°C. This sample was named “Ex. 7B”.

[0197]

In a similar manner, a DC power of 10 W was applied for 100 seconds to deposit the indium/tin oxide layer to a thickness of 10 nm while the substrate was kept at 170°C, after the electrical connection was changed to the indium/tin oxide target, and then a DC power of 100 W was put for 5 minutes to deposit the zinc oxide layer to a thickness of 100 nm, after the electrical connection was changed to the zinc oxide target and the substrate was heated to 250°C. This sample was named “Ex. 7C”.

[0198]

Ex. 7C was visually observed to have the intermediate layer finely separated, and this was confirmed by microscopic observation.

[0199]

Each sample was analyzed for its current-voltage characteristics in the same manner as in Example 3. The results are given in Table 22, where each of the characteristics is relative to that of Compar. 2-2.

[0200]

[Table 22]

	Jsc	FF	Voc	Eff.	Rsh
Ex. 7A/ Compar. 2-2	1.014	1.152	1.006	1.174	1.54×10^{2}
Ex. 7B/ Compar. 2-2	1.008	1.143	1.004	1.156	1.53×10^{2}
Ex. 7C/ Compar. 2-2	1.005	1.141	1.001	1.149	1.30×10^{2}

[0201]

Each of Ex. 7A, Ex. 7B and Ex. 7C had better characteristics than Compar. 2-2, and Ex. 7A was better than the others. The reliability test was also conducted in the same manner as in Example 3. The results are given in Table 23, where each of the characteristics reported is relative to the initial level.

[0202]

[Table 23]

	Jsc	FF	Voc	Eff.	Rsh
Ex. 7A	1.001	0.991	0.997	0.989	0.785
Ex. 7B	0.997	0.992	0.999	0.988	0.800
Ex. 7C	1.000	0.980	0.999	0.978	0.707
Compar. 2-2	0.959	0.906	0.992	0.862	0.387

[0203]

Each of Ex. 7A, Ex. 7B and Ex. 7C had higher reliability than Compar. 2-2.

[0204]

Ex. 7C had the finely separated intermediate layer, which, however, did not affect its reliability much. Ex. 7A had higher reliability than the others.

[0205]

To summarize these results: a higher conversion efficiency and reliability can be realized, when the zinc oxide layer was deposited at a lower temperature than the indium/tin oxide layer.

[Brief Description of the Drawings]

[0206]

[Fig. 1] A schematic cross-sectional view showing the structure of a conventional photovoltaic element provided with a zinc oxide layer.

[Fig. 2] A schematic cross-sectional view showing the electrical polarities of a part of one embodiment of the stacked photovoltaic element of the present invention.

[Fig. 3] A schematic cross-sectional view showing the structure of one embodiment of the stacked photovoltaic element of the present invention.

[Fig. 4] A schematic cross-sectional view showing the power-generating operation of the stacked photovoltaic element of the present invention.

[Fig. 5] A schematic view illustrating one embodiment of a suitable apparatus for producing a semiconductor layer for the stacked photovoltaic element of the present invention.

[Fig. 6] A schematic view illustrating one embodiment of a suitable apparatus for producing a zinc oxide layer for the stacked photovoltaic element of the present invention.

[Fig. 7] Schematic cross-sectional views showing the method of the present invention for producing a stacked photovoltaic element.

[Fig. 8] A schematic cross-sectional view showing the structure of one embodiment of the stacked photovoltaic element of the present invention.

[Fig. 9] A schematic cross-sectional view showing the structure of another embodiment of the stacked photovoltaic element of the present invention.

[Fig. 10] An explanatory view showing J-V curves of the stacked photovoltaic elements prepared in Example 3 and Comparative Example 2-1.

[Fig. 11] An explanatory view showing J-V curves of the stacked photovoltaic elements prepared in Example 3 and Comparative Example 2-2.

[Fig. 12] A schematic cross-sectional view showing the structure of the stacked photovoltaic element having an intermediate layer composed of one layer in Comparative Example.

[Description of Reference Numerals or Symbols]

[0207]

100 Stacked photovoltaic element

101 Substrate

102 Second photovoltaic element
103 Zinc oxide layer
104 First photovoltaic element
105 Transparent electrode
106 Short circuit in the second photovoltaic element
107 Short Circuit in the first photovoltaic element
200 Stacked photovoltaic element of the present invention
201 Substrate
202 Second zinc oxide layer showing layer of n- type electrical properties
203 First zinc oxide layer showing layer of n+ type electrical properties
204 First zinc oxide layer showing layer of n++ type electrical properties
205 Transparent electrode
206 Second photovoltaic element
207 Zinc oxide layer
208 First photovoltaic element
300 Stacked photovoltaic element of the present invention
301 Substrate
302 Second photovoltaic element
303 Second zinc oxide layer
304 First zinc oxide layer
305 First photovoltaic element
306 Transparent electrode

401, 403 Short circuit in the second photovoltaic element

402 Short circuit in the first photovoltaic element

500 Semiconductor deposited film forming apparatus

501 Load chamber

502 Chamber for n-layer

503 Chamber for i-layer of microcrystalline silicon

504 Chamber for i-layer of amorphous silicon

505 Chamber for p-layer

506 Unload chamber

507, 508, 509, 511 Gate valve

512 Heater for heating microcrystal i-layer of substrate

513 Plasma CVD chamber for microcrystal i-layer

514 Heater for heating n-layer of substrate

515 Plasma CVD chamber for n-type layer

516 Heater for heating i-layer of amorphous silicon of substrate

517 Plasma CVD chamber for i-layer

518 Heater for heating p-layer of substrate

519 Plasma CVD chamber for p-layer

520 Holder transporting rail

600 Sputtering chamber

601 Substrate holder

602 Gas inlet tube

603 Heater

604 Zinc oxide target

605 DC power source
606 Earth shield
700 Substrate
701 Reflection layer
702 Second photovoltaic element
703 Layer composed of indium oxide
704 Layer composed of zinc oxide
705 Intermediate layer
706 First photovoltaic element
800 Stacked photovoltaic element
801 Substrate
802 Light reflection layer
803 Second photovoltaic element
804 First layer composed of indium oxide
805 Second layer composed of zinc oxide
806 Intermediate layer
807 First photovoltaic element
808 Transparent electrode
900 Stacked photovoltaic element
901 Substrate
902 Light reflection layer
903 Second photovoltaic element
904 First layer composed of indium oxide
905 Second layer composed of zinc oxide
906 Intermediate layer
907 First photovoltaic element
908 Transparent electrode

1200 Stacked photovoltaic element

1201 Substrate

1202 Light reflection layer

1203 Second photovoltaic element

1206 Intermediate layer

1207 First photovoltaic element

1208 Transparent electrode

[Name of the Document] Abstract

[Abstract]

[Problem(s)] It is to provide a stacked photovoltaic element exhibiting a high conversion efficiency realized by producing large photocurrent without causing decreased electromotive force.

[Means for Solving the Problem(s)] A stacked photovoltaic element comprising a plurality of unit photovoltaic elements each composed of a pn- or pin-junction, connected to each other in series, wherein a zinc oxide layer is provided at least one position between the unit photovoltaic elements, and the zinc oxide layer has resitivity varying in the thickness direction.

[Elected Drawing] Fig. 3

【書類名】図面　{Name of Documents}　Drawings
【図１】　Fig.1

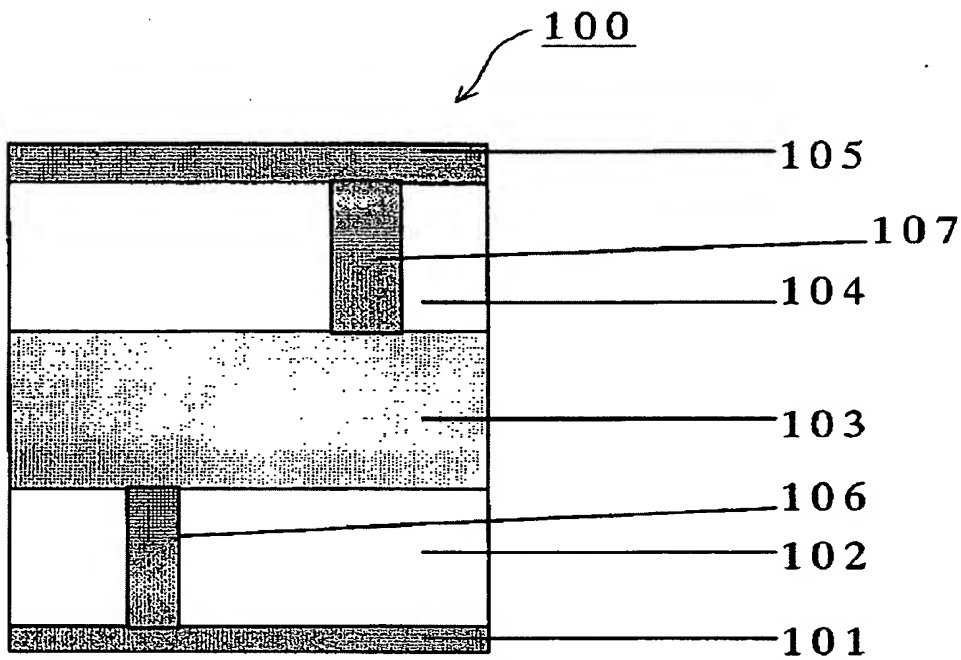

【図２】 Fig. 2

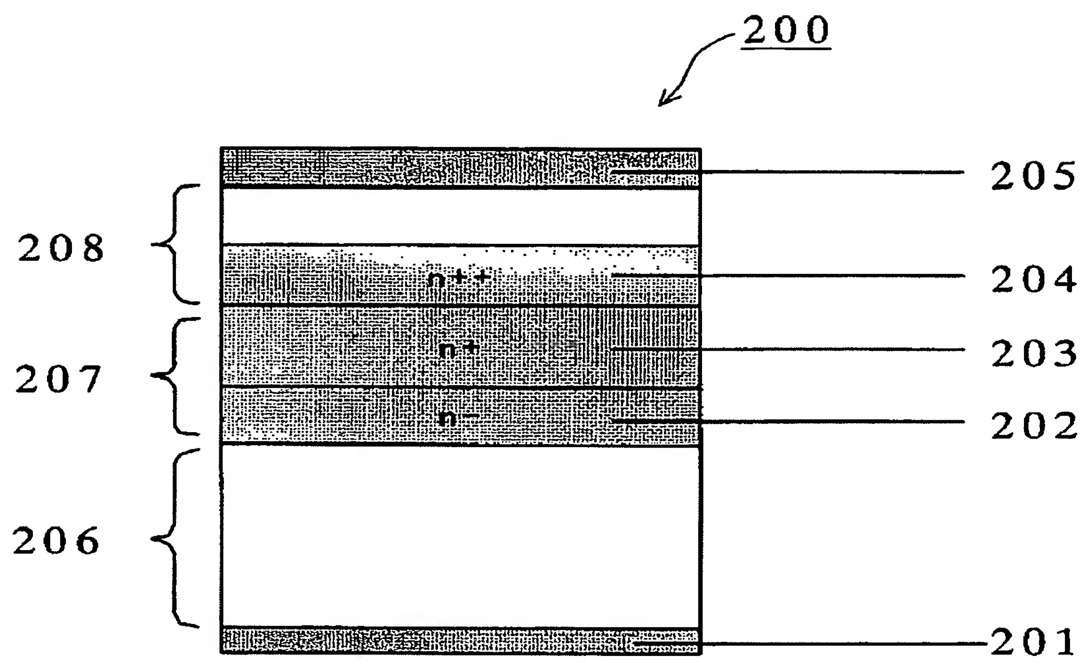

【図３】 Fig. 3

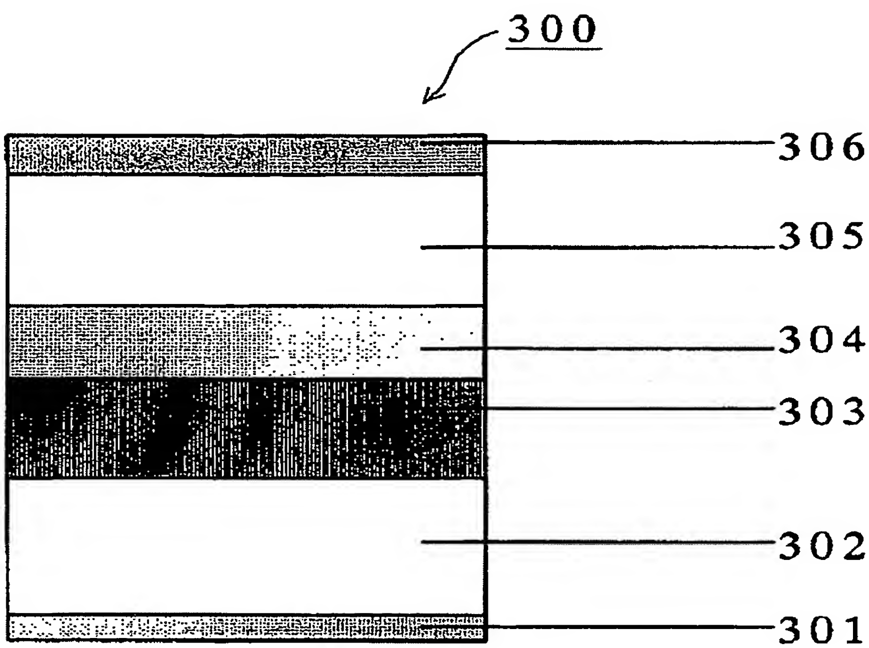

【図４】 Fig. 4

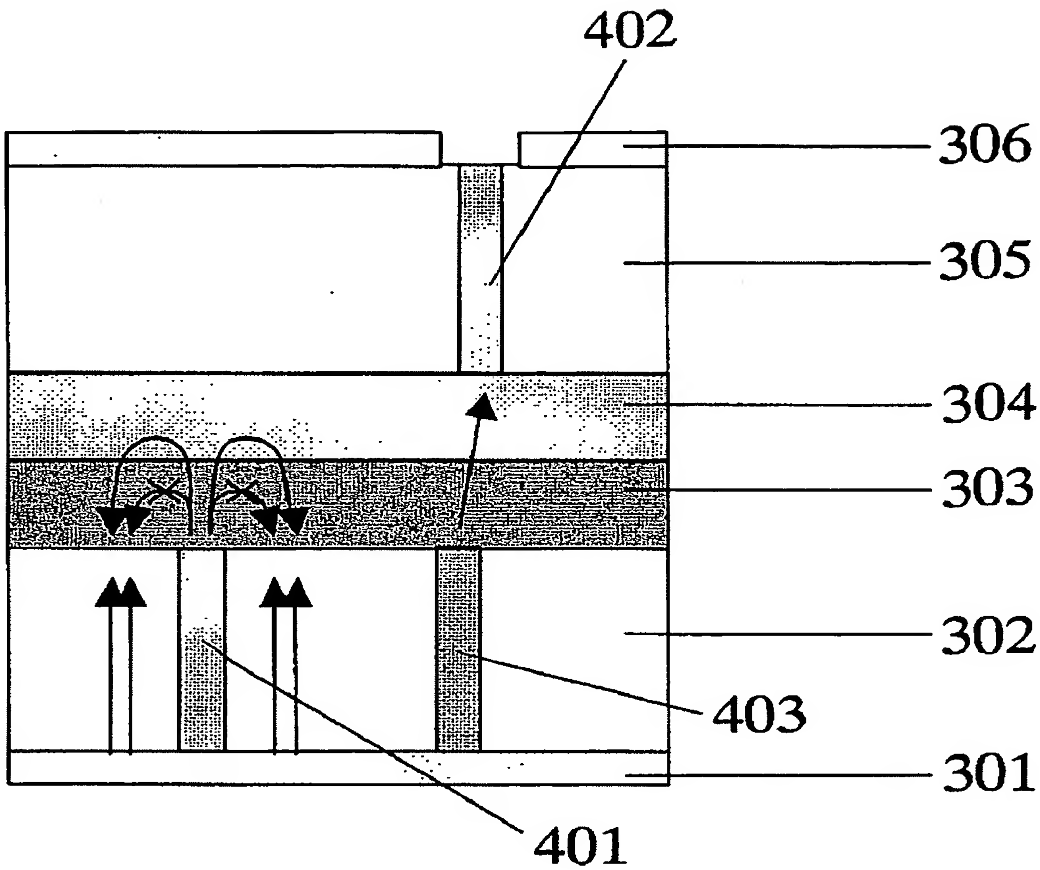

【図５】　Fig. 5

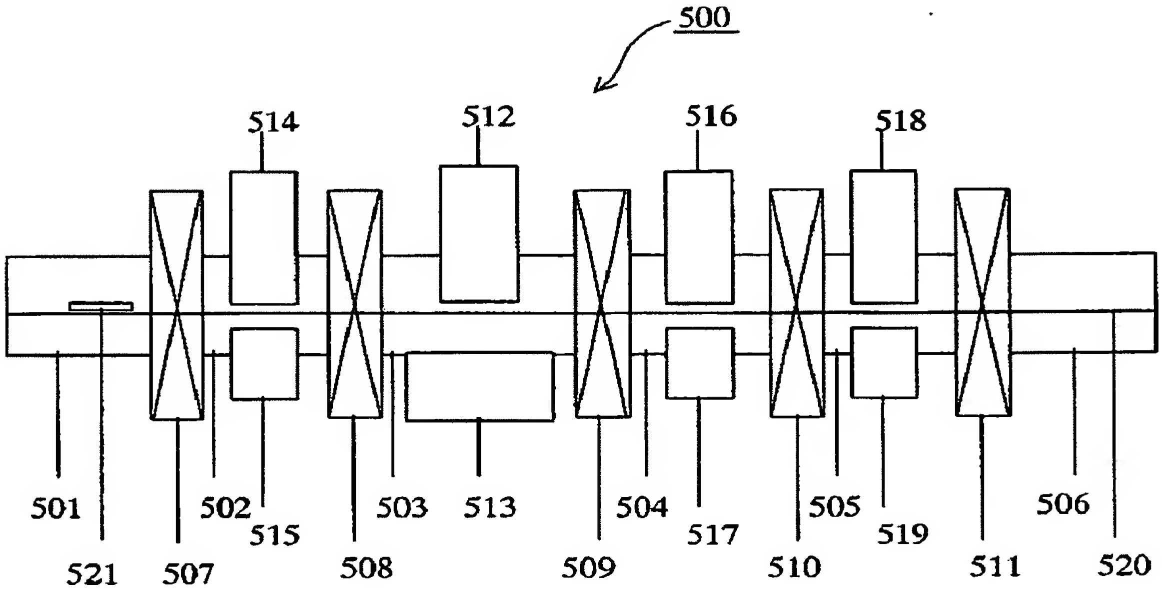

【図６】　Fig. 6

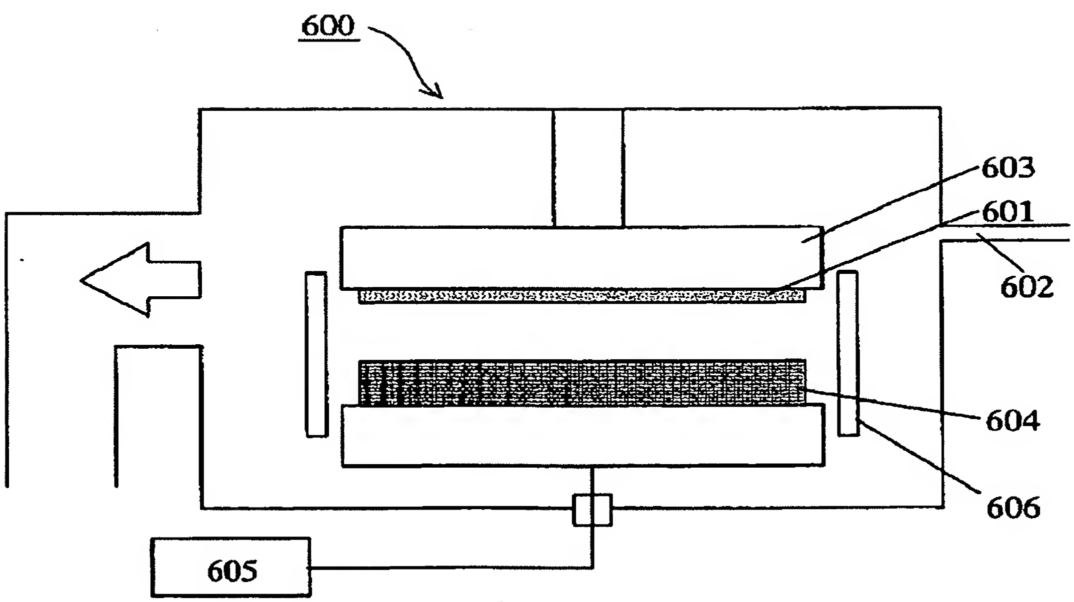

【図７】 Fig. 7

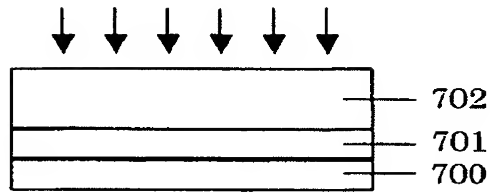

(a)酸化インジウムを含む層を堆積

A layer composed of indium oxide is deposited

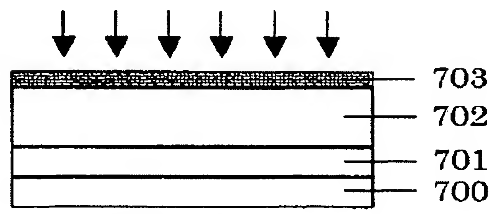

(b)酸化亜鉛を含む層を堆積

A layer composed of zinc oxide is deposited

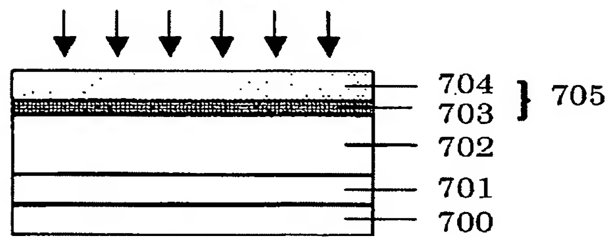

(c)光起電力素子を堆積

A photovoltaic element is deposited

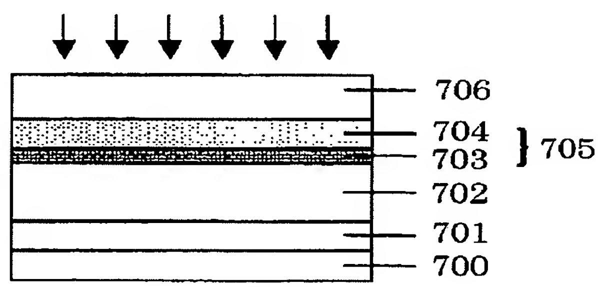

(d)透明電極を堆積

A transparent electrode is deposited

【図８】　Fig.8

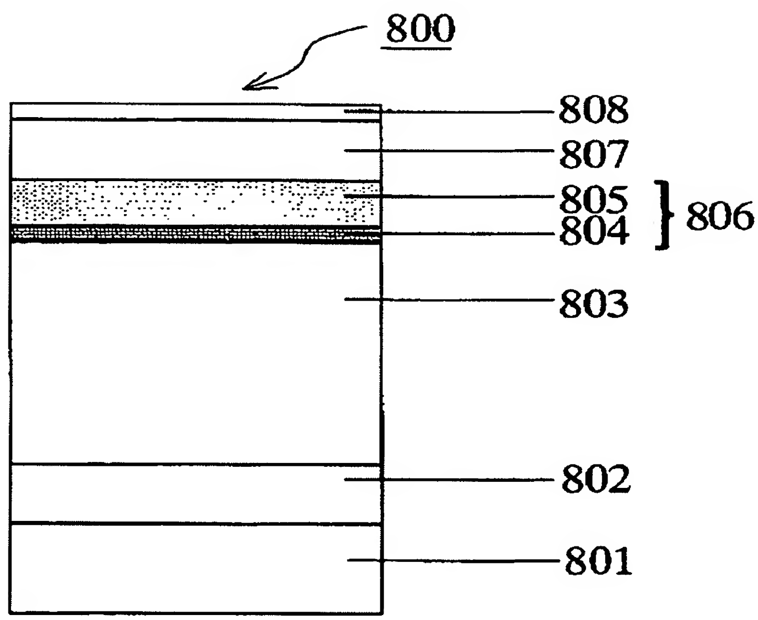

【図９】　Fig.9

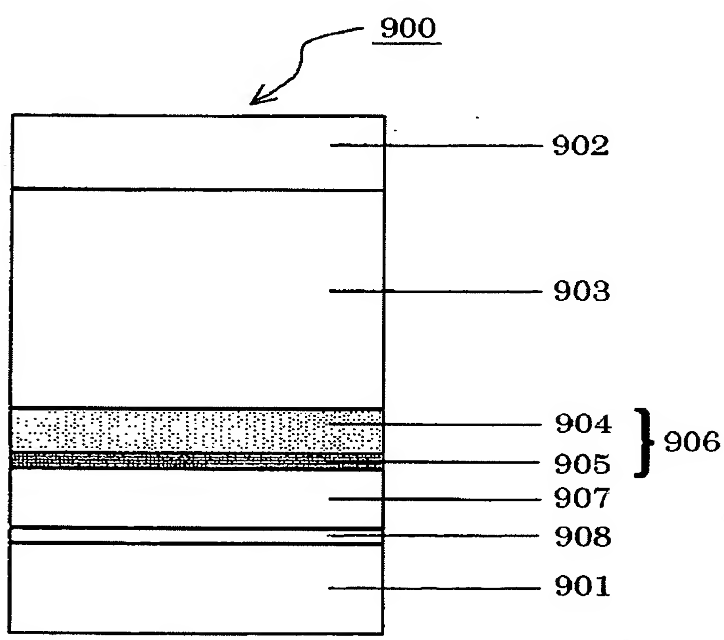

【図１０】　Fig. 10

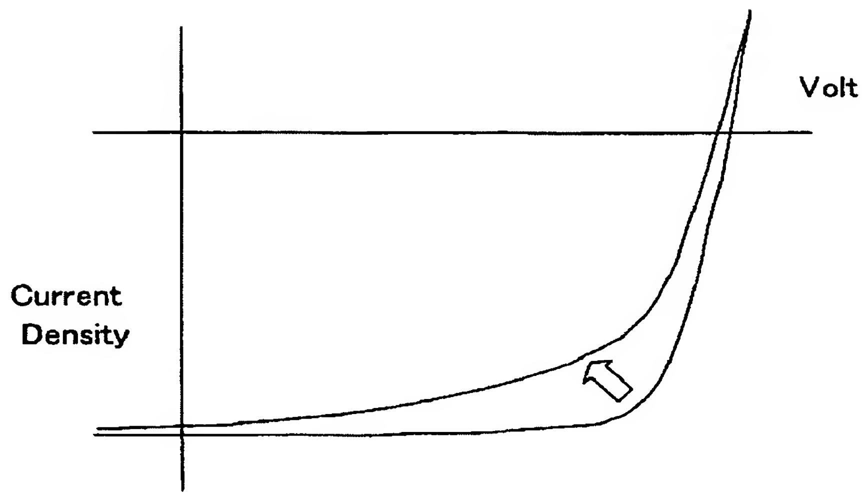

【図１１】　Fig. 11

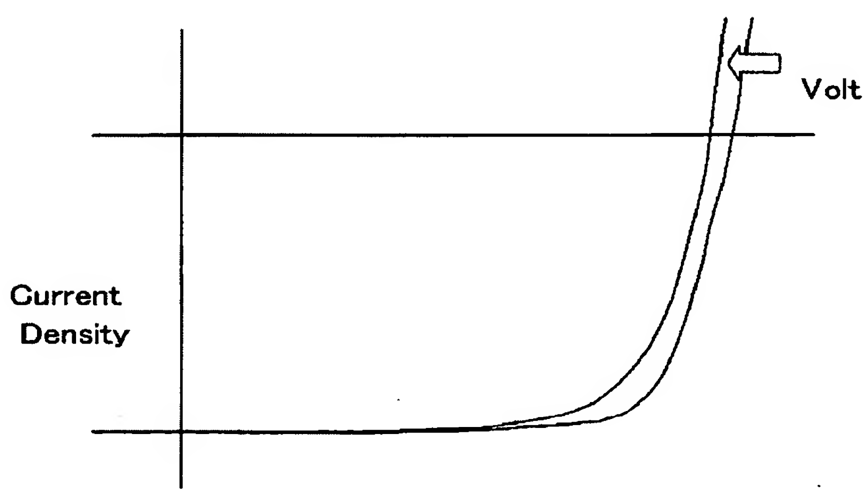

【図１２】　Fig. 12